Time-integrated four-wave mixing in GaN and ZnSe: Polarization-sensitive phase shift of the excitonic quantum beats

T. Aoki, G. Mohs,* Yu. P. Svirko, and M. Kuwata-Gonokami†
Department of Applied Physics, Faculty of Engineering, University of Tokyo and Cooperative Excitation Project of ERATO (JST), 7-3-1 Hongo, Bunkyo-ku, Tokyo 113-8656, Japan

(Received 11 August 2000; revised manuscript received 16 January 2001; published 9 July 2001)

We report on the study of quantum beats in the time-integrated four-wave mixing signal in reflection geometry from a pair of excitons with different valence orbitals in GaN and ZnSe. We observe a π-phase shift between quantum beats in the co- and cross-linear polarization configuration, and nearly 100% modulation of the signal for both materials. In the co-circular polarization configuration, the observed phases of the quantum beats at the frequency of the *A* exciton in GaN and heavy-hole exciton in ZnSe are 0.2π and 0.1π, respectively. The phases of the quantum beats change sign for co- and counter-circular polarization configurations and also for *A*- (heavy-hole) and *B*-(light-hole) excitons in GaN(ZnSe). We describe the third-order coherent optical response of the exciton pair with different valence orbitals by taking into account the finite memory depth of the four-particle correlation. In particular, our experimental findings indicate that excitons with different valence orbitals and equal angular momentum attract each other similar to excitons with the same valence orbitals but opposite angular momentum. Excitons with different orbitals and opposite angular momenta repel one another. The comparison between experimental and theoretical results allows us to develop a quantitative analysis of the four-particle correlation in the presence of an exciton pair with different valence orbitals. We show that the observed π-phase shift and nearly 100% modulation of the signal in the co- and cross-linear polarization configuration impose restraints on the memory functions, which describe the exciton-exciton interaction. These restraints imply, in particular, that electron spins play a more important role in the exciton-exciton interaction in comparison to hole spins. We show that a striking similarity, which we observe in the quantum beat signal from GaN and ZnSe, originates from the strong four-particle correlation contribution to the third-order excitonic nonlinearity.

DOI: 10.1103/PhysRevB.64.045212 PACS number(s): 71.35.Cc, 42.50.Md

I. INTRODUCTION

The strong potential of quantum beats for the study of dephasing processes has been widely recognized at the very beginning of quantum electronics. This effect, which indicates the presence of quantum coherence in the system, has been observed in the resonance fluorescence of two optical transitions with common ground state in mercury atoms.[1,2] Although there have been few observations of quantum beats of excitons in resonance fluorescence,[3] quantum beats have been studied extensively from the early 1990's in four-wave mixing (FWM) experiments in various semiconductors.[4–14] In these experiments, two excitons with different energies are excited by two short laser pulses delayed with respect to one another and the time-integrated (TI) FWM signal as a function of the time delay between the pulses shows oscillations with a period corresponding to the exciton energy difference. The first observation of this effect in the FWM signal from excitons has been reported in Ref. 4, where FWM in quantum wells (QW's) of variable width has been investigated. TI FWM measurements for a pair of excitons with different valence orbitals has been performed for the first time in GaAs QW's.[5,6] Here, *hh* and *lh* excitons excited by an ultrashort light pulse give rise to oscillations in the TI FWM signal with a period corresponding to the *hh*-*lh* splitting in the transmission spectrum.

The question whether these oscillations arise from the coupling of the excitonic transitions or from the interference of the signals from two independent oscillators (in other words, whether the observed effect is quantum beats or polarization interference[15]) was a central issue of the discussion for a long time. This is because although excitonic optical response may be described in spirit of atomic systems, the many-body origin of the excitonic nonlinearity makes discrimination of the quantum beats and the polarization interference a difficult experimental problem. The method, which is based on the dependence of the beating phase on the time delay between two pulses, has been proposed to diminish polarization interference and quantum beating in time-resolved (TR) FWM.[16] In the TI FWM, the quantum beats can be identified from the spectral dependence of the oscillating signal near the resonance.[18] In particular, it has been shown that in the case of the polarization interference no oscillations are observed in TI FWM signal at the exciton resonance frequencies. More recently, the problem of the origin of the oscillations in the FWM signal from a two-exciton system has been revisited because—in contrast to the polarization interference—the quantum beats of excitons is one of the manifestations of the mutual coherence of the electron-hole pairs due to the Coulomb-induced correlation among photoexcited carriers. Correspondingly, the study of the beating signal can provide us with important information on the many-particle correlation, the role of which in the nonlinear optical response at the band edge has become widely recognized. In particular, by utilizing the method developed in Ref. 16, it has been shown[17] that when the TR FWM signal in GaAs-$Al_xGa_{1-x}As$ multiple quantum well is produced by

pulses of the same circular polarization, the dynamic beating behavior at the hh-lh frequency provides evidences of the four-particle correlation contribution to the third-order nonlinearity. In order to study the four-particle correlation by using the TI FWM technique, we have proposed the method, which utilizes dependence of the fourth- and higher-order correlations on the carriers spin.[19] Such dependence gives rise to a sensitivity of the amplitude and phase of the quantum beats to the polarization configuration, i.e., on the polarization of the light waves involved in the FWM process.[19]

The polarization dependence of quantum beats has been reported in Ref. 7, where the quantum beats between hh and lh excitons in GaAs quantum wells have been studied for parallel and orthogonal linear polarized incident pulses. These polarization configurations of the TI FWM experiment are referred to as co- and cross-linear polarization configurations, respectively. The observed π phase shift, which has been accompanied by a lower intensity and faster decay in the cross-linear compared to the colinear polarization configuration, is the most prominent feature of the beating signal. The experiment[7] has been interpreted in the spirit of atomic systems using a six-level model, which accounts for the spin degree of freedom of the carriers in the conduction and valence bands. The model allows to reproduce the π phase shift when changing the polarization configuration from co- to cross-linear. However, since this model is based on the one-electron picture, it may not be employed to study many-body effects, which have become of particular interest recently.

Our recent experiments have revealed that the phase of the quantum beats at positive time delays is determined by the interplay of various mechanisms of the third-order nonlinearity at the fundamental band edge.[12,19] This makes phase measurements a suitable tool for studying four-particle correlation effects[20–24] in the third-order optical response of semiconductors. In the spectral window close to the exciton resonance the effects of four particle correlation, which originate from the Coulombic interaction between photogenerated carriers and the Pauli exclusion principle, can be classified in terms of a spin-dependent interaction between excitons.[25–28] In particular, the weakly interacting boson model,[28] in which the interaction between $1s$ excitons is described by using two parameters to acount for excitons with different angular momenta, has allowed us to reproduce the overall features of polarization-sensitive FWM spectra. Recently, we have extended this model to describe the TI FWM signal from a pair of excitons with different valence orbitals in GaN.[19] In this model, we have suggested that the major contribution to the third-order nonlinearity originates from the continuum of unbound two-exciton states assuming that the interaction between excitons is instantaneous. However, the description of the TI FWM experiment requires an extension of this model to elucidate the role of non-Markovian memory effects[29,30] in the exciton-exciton interaction and, in particular, the role of the long-living correlation between carriers, which are associated with the bound two-exciton states.[25–28]

In this paper, we report the observation of polarization-sensitive quantum beats from excitons in GaN and ZnSe. In order to clarify the exciton-exciton interaction effects in the nonlinear optical response we perform precise measurements of the phase of the quantum beats in various polarization configurations. This allows us to investigate the role of the electron and hole spin in the four-particle correlations. We interpret our experimental findings by developing a theory based on the third-order optical response of the two-exciton system accounting for a finite correlation time of the exciton interaction. The analysis of the experimental data allows us to conclude that the interaction between excitons depends mainly on the electron spin rather than on hole spin. This may considerably simplify the description of the temporal evolution of the 2ω coherence in the continuum of two-exciton states, which can be studied by time-resolved FWM spectroscopy.

The reminder of the paper is organized as follows. In the next section, we present the results of our measurements on quantum beats in the TI FWM signal associated with pairs of excitons with different valence orbitals in GaN and ZnSe. In Sec. III we discuss our experimental findings in terms of the evolution equation for the coherent excitonic polarization. This equation, which accounts for a finite memory depth of the four-particle correlation, is derived in the Appendix, where we present a phenomenological theory of the coherent third-order optical response at the semiconductor band edge in the presence of two excitons with different valence orbitals. By assuming that the incident pulses are much shorter than the exciton dephasing time and beating frequency, we calculate the amplitude of the excitonic polarization at the frequencies of the excitons and, correspondingly, the intensity of the TI FWM signal. In Sec. III, we obtain constrains imposed by the $\chi^{(3)}$ regime on the amplitudes and phases of the quantum beats in different polarization configurations. By taking the finite correlation memory time of the exciton-exciton interaction into account, we extend the treatment of the polarization-sensitive TI FWM measurements in GaN presented in Ref. 19. In particular, we show implications of our experimental findings on properties of the memory functions, which describe the interaction between excitons. We show that in the short-memory approximation, i.e., when the unbound two-exciton states dominate the third-order optical response of the system, the phase of the quantum beats is determined by both exciton-exciton interaction and excitation induced dephasing (EID). In Sec. IV we summarize our experimental and theoretical results.

II. EXPERIMENT

We perform FWM measurements in GaN and ZnSe crystals. GaN is grown by hydride vapor phase epitaxy on a sapphire substrate to a thickness of about 220 μm.[31] The sapphire substrate is removed after growth. ZnSe is grown by molecular-beam epitaxy on a (100) surface of a GaAs substrate to a thickness of 500 Å . The samples are mounted in a closed-cycle helium cryostat and kept at 12 K. The linear reflection spectra reveal *A*- and *B*-exciton resonances in GaN at 356.3 nm and 355.8 nm, respectively, and light- and heavy-hole exciton resonances in ZnSe at 439.7 nm and 441.5 nm, respectively.

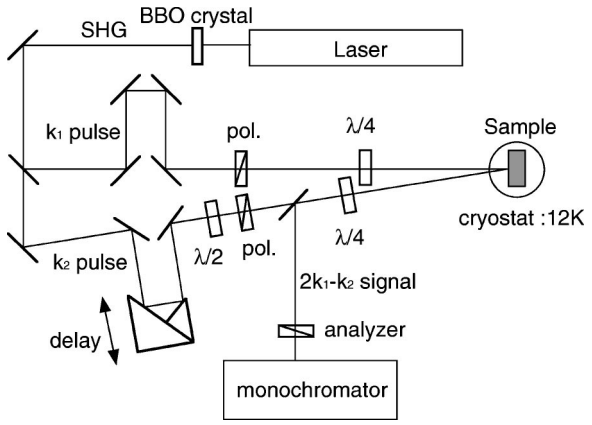

FIG. 1. Experimental setup.

A sketch of the experimental setup is shown in Fig. 1. In our FWM measurements we use a frequency-doubled Kerr-lens mode-locked Ti-sapphire laser, which produces 120 fs pulses at a repetition rate of 76 MHz. In the experiments with the GaN and ZnSe crystals, second-harmonic pulses, which are generated by a beta-barium borate (BBO) or a lithium tribonate (LBO) crystal, respectively, excite both excitons simultaneously.

We use two-pulse TI FWM in reflection geometry. In this geometry, two pulses with wave-vectors $\mathbf{k}_1$ and $\mathbf{k}_2$ are incident on the sample with $\mathbf{k}_1$ normal to the sample surface. The FWM signal in the direction $2\mathbf{k}_1-\mathbf{k}_2$ traces back the incident path of the $\mathbf{k}_2$ pulse and is reflected at a half-mirror set in the $\mathbf{k}_2$ path. The signal is time integrated and spectrally resolved by a monochromator. This allows us to detect the signal at the frequency of each exciton resonance separately.

We use five polarization configurations, which will hereafter be abbreviated by superscript (pts) according to the polarization of the incident pump pulse (p) with wave-vector $\mathbf{k}_1$, the test pulse (t) with wave-vector $\mathbf{k}_2$, and the signal pulse (s) with wave-vector $2\mathbf{k}_1-\mathbf{k}_2$. Correspondingly, in the (xxx) configuration, the two incident pulses and the signal pulse are linearly polarized along the x direction (this configuration is also referred to as the colinear configuration). In the (xyy) configuration, the pump pulse with wave-vector $\mathbf{k}_1$ is linearly polarized along the x direction, while the test pulse with wave-vector $\mathbf{k}_2$ and the signal pulse are linearly polarized along the y direction (cross-linear configuration). Similarly, in the $(+++)$ configuration, the pump, test, and signal pulses are σ_+ polarized (co-circular configuration), in the $(x++)$ configuration, the pump pulse is x polarized, while the test and signal pulses are σ_+ polarized, and, finally, in the $(x+-)$ configuration, the pump pulse is x polarized, the test pulse is σ_+ polarized, and the signal pulse is σ_- polarized. In the $(x++)$-configuration, a $\lambda/4$ plate turns the polarization of the $\mathbf{k}_2$ pulse σ_+, and additionally turns the polarization of σ_+ signal pulse to the y direction on its pass back. Therefore, a σ_+ component can be selectively measured by passing the signal though an analyzer before detection. In the $(x+-)$ configuration, the signal is detected similarly by turning the analyzer 90 degrees with respect to the $(x++)$ configuration.

The zero position of the time delay T between the two incident pulses is determined by monitoring the signal in the directions $2\mathbf{k}_1-\mathbf{k}_2$ and $2\mathbf{k}_2-\mathbf{k}_1$, which are equivalent yet reversed with respect to T. The symmetry point of the two traces is defined as $T=0$. By examining the dependence of the signal intensity on the excitation power, we confirm that all the measurement are performed strictly in the $\chi^{(3)}$ regime.

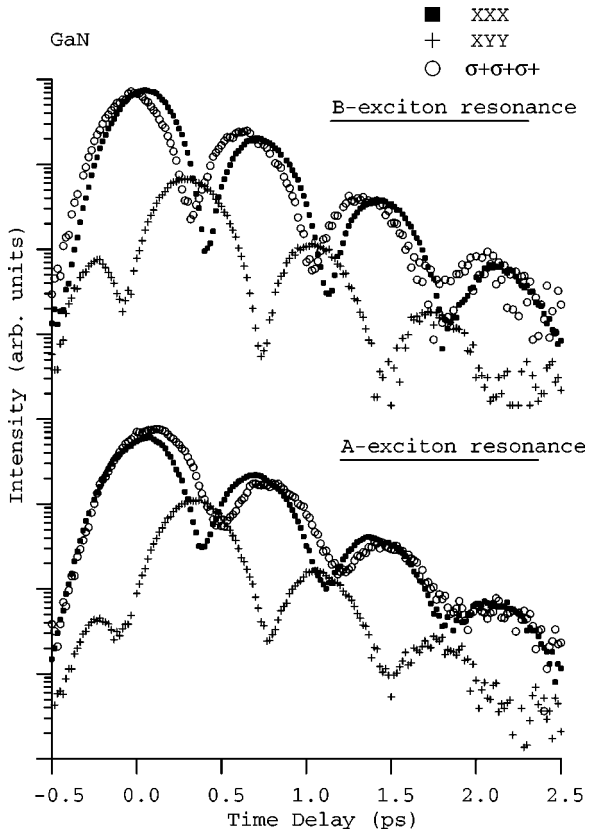

FIG. 2. TI FWM signal in GaN in the direction $2\mathbf{k}_1-\mathbf{k}_2$ as a function of time delay T at the A- and B-exciton resonance for the colinear (■), cross-linear (+), and co-circular (○) polarization configuration. Positive time delay is defined as pulse $\mathbf{k}_2$ arriving first.

Figures 2(a) and 2(b) show the TI FWM signal in GaN at the frequency of the A and B excitons, respectively, as a function of the delay T in the (xxx), (xyy), and $(+++)$ configuration. The TI FWM signal in the (xxx), $(x++)$, and $(x+-)$ configuration is presented in Figs. 3(a) and 3(b). The results of the measurements in the (xxx) configuration are shown in both figures to enable an easy comparison between the relative magnitudes of the signal. In particular, one can observe that the magnitude of the signal in the (xxx), (xyy), and $(+++)$ configurations is several times larger than that in the $(x++)$ and $(x+-)$ configurations.

One can see from Figs. 2 and 3 that the TI FWM signal in all configurations shows a typical quantum beats behavior. At $T>0$, the overall TI FWM signal intensity shows an exponential decay with the exciton dephasing rate, and oscillates with a frequency given by the energy difference between the A and B excitons. One may notice that a local maximum in the (xxx) configuration coincides with a local minimum in the (xyy) configuration, and at $T=0$, the signal

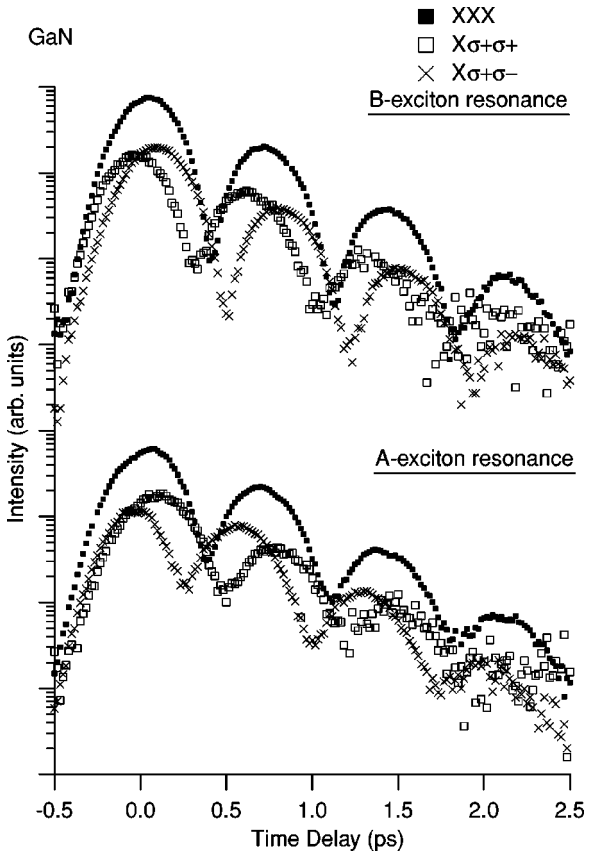

FIG. 3. TI FWM signal in GaN in the direction $2\mathbf{k}_1-\mathbf{k}_2$ as a function of time delaty T at the A- and B-exciton resonance; □ $-(x++)$ polarization configuration; × $-(x+-)$ polarization configuration; ■ $-(xxx)$ polarization configuration.

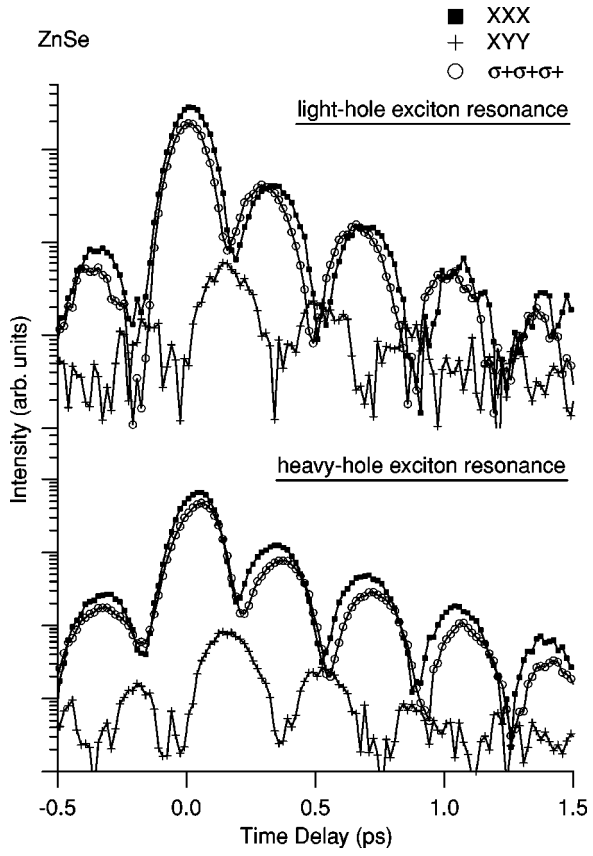

FIG. 4. TI FWM signal in ZnSe as a function of time delay T at the light-hole and heavy-hole exciton resonance for the colinear (■), cross-linear (+), and co-circular (○) polarization configuration. The solid line provides guidance for the eye.

magnitude is maximum in the (xxx) configuration and minimum in the (xyy) configuration.

By representing the magnitude of the TI FWM signal as $I^{pts}_{A,B}\propto[1+a^{pts}_{A,B}\cos(\Delta T-\phi^{pts}_{A,B})]\exp(-2\gamma T)$, where subscripts ''$A$'' and ''$B$'' indicate A and B excitons in GaN and hh and lh excitons in ZnSe, respectively, and superscripts (pts) label the polarization configuration (Δ and γ are the beat period and exciton dephasing rate), one can conclude that the phase of the signal in the (xxx) and (xyy) configurations is 0 and π, respectively, for both excitons. Correspondingly, the beats in the (xxx) and (xyy) configuration show a $\cos^2$- and $\sin^2$-like behavior, respectively, because the modulation depth in these configurations is as high as 95%: $a^{xxx}_{A,B}\approx a^{xyy}_{A,B}\approx 0.95$.

In the $(x++)$ and $(x+-)$ configuration (see Fig. 3), the TI FWM signal has neither a maximum nor a minimum at $T=0$, and thus, the phase of the quantum beats is neither 0 nor π. Furthermore, the phase of the beats is different for signals measured at the A- and the B-exciton resonance. One can also see that in the $(x++)$ and $(x+-)$ configuration, the modulation of the signal is considerably less than in the co- and cross-linear configurations: $a^{x++}_{A,B}\approx a^{x+-}_{A,B}\approx 0.8$.

Figures 4 and 5 show the TI FWM signal in ZnSe in the (xxx), (xyy), and $(+++)$ configuration and in the (xxx), $(x++)$, and $(x+-)$, respectively. One can observe from the graphs that the polarization-sensitive TI FWM for light- and heavy hole excitons in ZnSe shows a similar behavior as for A and B excitons in GaN.

One may notice that the decay time of the TI FWM signal is almost same in all polarization configurations. Such insensitivity of the dephasing to the polarization configuration indicates that inhomogeneous broadening[32] does not play an important role in the phenomena we study in our experiment, i.e., both GaN and ZnSe samples are homogeneously broadened.[12,21,33] One may recall that in the case of a homogeneously broadened system, the signal is emitted in the form of a free induction decay. Since this is equivalent for both the co- and cross-linear polarization configurations, the same decay rate should be expected. In the case of an inhomogeneously broadened system, on the other hand, the signal is emitted in the form of a photon echo. Therefore, from the arrival of the test pulse at time τ up to the signal emission at time 2τ the system is in one-exciton states for the colinear and in two-exciton states for the cross-linear polarization configurations, respectively. Correspondingly, in the presence of inhomogeneous broadening, the decay rate for the cross-linear polarization configuration is faster than that for the colinear, reflecting the faster two-exciton states dephasing.

The results of our phase measurements of the beating signal in GaN and ZnSe are summarized in Table I. $\phi^{pts}_{A,B}$ is

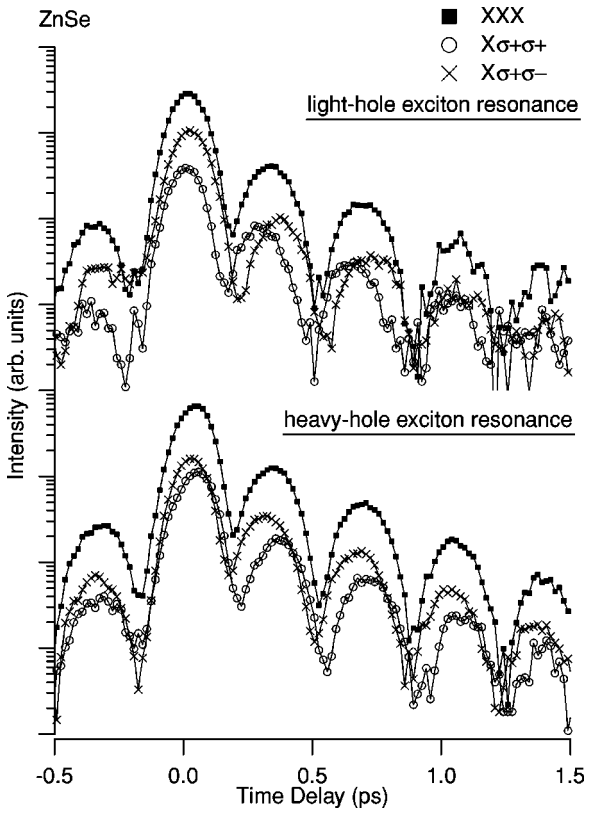

FIG. 5. TI FWM signal in ZnSe as a function of time delay T at the light hole and heavy hole and exciton resonance; $\bigcirc-(x++)$ polarization configuration; $\times-(x+-)$ polarization configuration; $\blacksquare-(xxx)$ polarization configuration. The solid line provides guidance for the eye.

obtained by fitting the experimental data for different polarization configurations. By using the weakly interacting boson model we have shown in Ref. 19 that the amplitude and phase of the beating signal in GaN are determined by the interplay of excitation-induced dephasing (EID) and the polarization-sensitive interaction within the continuum of unbound exciton states. In the next section, we extend this treatment of the TI FWM by accounting for memory effects in the polarization-sensitive exciton-exciton interaction.

III. THEORY AND DISCUSSION

A. TI FWM signal in the $\chi^{(3)}$ regime

We have shown in the previous section, that the TI FWM signal in both GaN and ZnSe shows similar features indicating that in the $\chi^{(3)}$ regime, the quantum beats are determined by fundamental mechanisms of optical nonlinearity at the band edge, where four-particle correlation effects play a crucial role. In this section, by extending the treatment of the excitonic nonlinearity in terms of a polarization-sensitive exciton-exciton interaction[19,34–37] we will analyze the results of our phase measurements accounting for memory effects. By using the evolution equation for the excitonic polarization, which is derived in the Appendix, we analyze properties of the TI FWM signal in the $\chi^{(3)}$ regime. This allows us to obtain certain restraints, which our experimental findings impose on the memory functions.

We assume that there are two exciton resonances with different valence orbitals, which will be labeled below by subscripts A and B. They are excited by a laser pulse with central frequency ω. We start from the equation of motion for the complex amplitudes of the right- and left-circular components of the excitonic polarization at that frequency. Following Ref. 34 we introduce normalized excitonic polarizations associated with the A and B excitons $p_{A,B\pm}=<b_{A,B\pm}>/(Vv_{A,B})^{1/2}$, where $b_{A,B\pm}$ are the corresponding exciton annihilation operators (subscripts $\pm$ denote circular polarizations), $v_{A,B}$ are the effective exciton volumes, and V is the crystal volume. With an account for terms up to the third order in the light field, the temporal evolution of $p_{A\pm}$ can be described by the following equation, which is obtained in the Appendix:

$$
\begin{aligned}
&-i\frac{\partial p_{A\pm}}{\partial t}+\Delta_A p_{A\pm}\\
&\quad=E_\pm-\left(C_A|p_{A\pm}|^2+\frac{1}{2}\sqrt{\frac{v_A}{v_B}}C'|p_{B\mp}|^2\right)E_\pm-\frac{1}{2}\sqrt{\frac{v_A}{v_B}}C'p^*_{B\mp}p_{A\pm}E_\mp-p^*_{A\pm}\int_0^\infty F_{AA}(\tau)p^2_{A\pm}(t-\tau)e^{-2i\Delta_A\tau}d\tau\\
&\quad-p^*_{B\pm}\sqrt{\frac{v_A}{v_B}}\int_0^\infty F_{AB}(\tau)p_{A\pm}(t-\tau)p_{B\pm}(t-\tau)e^{-i(\Delta_A+\Delta_B)\tau}d\tau-p^*_{A\mp}\int_0^\infty G_{AA}(\tau)p_{A\pm}(t-\tau)p_{A\mp}(t-\tau)e^{-2i\Delta_A\tau}d\tau\\
&\quad-p^*_{B\mp}\sqrt{\frac{v_A}{v_B}}\int_0^\infty G_{AB}(\tau)p_{A\pm}(t-\tau)p_{B\mp}(t-\tau)e^{-i(\Delta_A+\Delta_B)\tau}d\tau. \qquad (1)
\end{aligned}
$$

Here $\Delta_{A,B}=\omega_{A,B}-\omega-i\gamma$, $\omega_{A,B}$, and γ are the exciton frequencies and dephasing rate, respectively, and $E_\pm$ are the Rabi frequencies, which are proportional to the product of the amplitudes of the right- and left-circular polarized components of the electric field at the frequency ω and the effective interband dipole moment (see the Appendix). The evolution equation for $p_{B\pm}$ can be obtained by replacing subscript A with B and vice versa in Eq. (1).

TABLE I. Measured phase of the quantum beats for each polarization configuration at each resonance. A phase offset of 0.1π due to the finite pulse width has been subtracted for the numbers in brackets.

Polarization configuration	Phase			
	GaN		ZnSe	
	ϕ_A	ϕ_B	ϕ_{hh}	ϕ_{lh}
(xxx)	0.1π (0.0π)	0.1π (0.0π)	0.1π (0.0π)	0.0π (-0.1π)
(xyy)	-0.9π (1.0π)	-0.9π (1.0π)	-0.9π (1.0π)	-0.9π (1.0π)
$(+++)$	0.4π (0.3π)	-0.1π (-0.2π)	0.2π (0.1π)	-0.2π (-0.3π)
$(x++)$	0.4π (0.3π)	-0.1π (-0.2π)	0.2π (0.1π)	-0.2π (-0.3π)
$(x+-)$	-0.2π (-0.3π)	0.4π (0.3π)	-0.1π (-0.2π)	0.2π (0.1π)

The first term on the right-hand side of Eq. (1) gives the linear optical response of the A exciton at the frequency ω, while the second and third term describe the phase-space filling (PSF) effect.[38] The PSF parameters C and C', which are introduced in the Appendix, account for the reduction of the exciton-photon coupling due to the existing exciton population in the medium.

The last four terms on the right-hand side of (1) describe the effects of the 2ω coherence in the nonlinear response of the two-exciton system. The 2ω coherence, which is due to the presence of bound and unbound two-exciton states, is determined by first- and higher-order exciton-exciton interaction effects. The memory functions $F_{AA}(\tau)$ and $G_{AA}(\tau)$ describe the 2ω coherence, which is associated with the interaction between two excitons of the A valence orbital (A excitons) with equal and opposite angular momentum, respectively. Similarly, the memory functions $F_{AB}(\tau)$ and $G_{AB}(\tau)$ describe the 2ω coherence due to the interaction between excitons of different valence orbitals (A and B excitons) with equal and opposite angular momentum, respectively.

The characteristic time of the memory functions are determined by the memory depth of the four-particle correlation. In the meanfield approximation, when only instantaneous interaction between excitons with the same spin and the same energy is allowed,[39] $F_{AA,BB}=R_{A,B}\delta(\tau)$, $F_{AB}(\tau)=G_{AA}(\tau)=G_{AB}(\tau)=0$ and $C'=0$, Eq. (1) reduces to the modified semiconductor Bloch equation [see Eq. (A11) in the Appendix]. If the long-living 2ω coherence, i.e., the bound biexcitons, plays an important role in the nonlinear optical response, the memory functions should have pronounced harmonic components, oscillating with the frequencies corresponding to the relevant biexciton binding energies. For example, when only the interaction between A excitons with opposite angular momentum is allowed, the memory function $G_{AA}(\tau)$ may be reduced to $G_{AA}(\tau)\propto W\delta(\tau)-iK\exp\{i\omega_b\tau\}$, where ω_b is the biexciton binding energy.[34]

We assume that the incident light pulses of the duration τ_p with wave-vectors $\mathbf{k}_{1,2}$ are shorter than the exciton coherence time and use the δ-function approximation for the incident electric field:

$$E_{\pm}=E_{1\pm}\delta\left(\frac{t-\tau_1}{\tau_p}\right)\exp\{i\mathbf{k}_1\mathbf{r}\}+E_{2\pm}\delta\left(\frac{t-\tau_2}{\tau_p}\right)\exp\{i\mathbf{k}_2\mathbf{r}\}. \tag{2}$$

In this paper, we will consider the case of $\tau_2<\tau_1$, i.e., the pulse with the wave-vector $\mathbf{k}_2$ arrives first. The time-integrated FWM signal

$$I^{pts}_{A,B}(T)\propto\int_{-\infty}^{+\infty}|p^{(3)pts}_{A,B}(t)|^2dt, \tag{3}$$

can be presented in the following form at positive time delay ($T=\tau_1-\tau_2>0$):

$$I^{pts}_{A,B}(T)\propto[I^{pts}_{0A,B}+\mathrm{Re}\{S^{pts}_{A,B}\}\cos\Delta T\pm\mathrm{Im}\{S^{pts}_{A,B}\}\sin\Delta T]e^{-2\gamma T}. \tag{4}$$

Here, $\Delta=\omega_B-\omega_A$, while $I^{pts}_{0A,B}$ and $S^{pts}_{A,B}$ are determined by the memory functions (see Appendix).

Equation (4) indicates that the phases of the quantum beats at the frequency of the A and B exciton have opposite signs. As one can observe from Figs. 2–5 this well corresponds to our experimental findings for all polarization configurations. Moreover, by using the definitions of $I^{pts}_{0A,B}$ and $S^{pts}_{A,B}$ from the Appendix, one can find that the $\chi^{(3)}$ regime imposes the following constrains (compare with Ref. 28):

$$2(I^{x++}_{0A,B}+I^{x+-}_{0A,B})=I^{xxx}_{0A,B}+I^{xyy}_{0A,B}, \tag{5}$$

$$2(S^{x++}_{A,B}+S^{x+-}_{A,B})=S^{xxx}_{A,B}+S^{xyy}_{A,B}. \tag{6}$$

These constrains, which are due to the third-order nature of the nonlinear effect, also hold in our experiment.

B. Comparison with the results of the phase measurements

In this section, we will analyze the experimental results, which have been presented in Sec. II, in terms of Eq. (4) for the TI FWM signal. By using the expressions for $I^{pts}_{0A,B}$ and $S^{pts}_{A,B}$ obtained in the Appendix, we show that our experimental findings allow us to obtain the relationship between memory functions.

Let us start from the results of the phase measurements. In the (xxx) and (xyy) configuration, the observed phase of the quantum beats is 0 and π, respectively, for both excitons (see Fig. 2). Therefore, from Eq. (4), we can conclude that in these polarization configurations $\mathrm{Im}\{S^{xxx}_{A,B}\}=\mathrm{Im}\{S^{xyy}_{A,B}\}=0$. Moreover, the zero phase of the beating signal in the (xxx) configuration implies $\mathrm{Re}\{S^{xxx}_{A,B}\}>0$, while the π phase shift in the (xyy) configuration gives $\mathrm{Re}\{S^{xyy}_{A,B}\}<0$.

In the $(x++)$ and $(x+-)$ configuration, the beating phase is neither 0 nor π and, therefore, Eq. (4) does not impose any constrains on $S_{A,B}^{x++}$ and $S_{A,B}^{x+-}$. However, constrains (5) and (6), along with the π phase shift between the beating signals in the (xxx)- and (xyy)-configuration allow us to obtain information on the properties of the TI FWM signal in the $(x++)$ and $(x+-)$ configuration. Specifically, since $\mathrm{Im}\{S_{A,B}^{xxx}\}=\mathrm{Im}\{S_{A,B}^{xyy}\}=0$, Eq. (6) results in $\mathrm{Im}\{S_{A,B}^{x++}\}=-\mathrm{Im}\{S_{A,B}^{x+-}\}$.

In order to interpret the results of the experiment further, we consider the modulation depths. One can observe from Fig. 2 that the modulation depth of the signal in the (xxx) and (xyy) configuration is much higher than that in the $(x++)$ and $(x+-)$ configuration. Specifically, in the (xxx) configuration, we find nearly 100% modulation of the TI FWM signal, i.e., $a_{A,B}^{xxx}\approx a_{A,B}^{xyy}\approx 0.95$. Therefore, in a first approximation $\mathrm{Re}\{S_{A,B}^{xxx}\}=I_{0A,B}^{xxx}$ and $\mathrm{Re}\{S_{A,B}^{xyy}\}=-I_{0A,B}^{xyy}$ and, therefore, the signal in (xxx) and (xyy) configuration can be represented in the following form: $I_{A,B}^{xxx}(T)\propto I_{0A,B}^{xxx}(1+\cos\Delta T)e^{-2\gamma T}$ and $I_{A,B}^{xyy}(T)\propto I_{0A,B}^{xyy}(1-\cos\Delta T)e^{-2\gamma T}$.

The 100%-modulation depth and the π phase shift of the TI FWM signal in the (xxx) and (xyy) configuration impose severe restrictions on the amplitude and phase of the signal in the $(x++)$ and $(x+-)$ configuration. Specifically, definitions (A19)–(A24) from the Appendix allow one to arrive at the following equations:

$$I_{A,B}^{x++}(T)\propto[I_{0A}^{x++}+\mathrm{Re}\{S_A^{x++}\}\cos\Delta T \pm \mathrm{Im}\{S_A^{x++}\}\sin\Delta T]e^{-2\gamma T}, \tag{7}$$

$$I_{A,B}^{x+-}(T)\propto[I_{0A}^{x++}+\mathrm{Re}\{S_A^{x++}\}\cos\Delta T \mp \mathrm{Im}\{S_A^{x++}\}\sin\Delta T]e^{-2\gamma T}. \tag{8}$$

Therefore, the phase of the quantum beats in the TI FWM signal in the $(x++)$ and $(x+-)$ configuration in the $\chi^{(3)}$ regime have an opposite sign but the same magnitude for A and B excitons:

$$\phi_A^{x++}=-\phi_A^{x+-}=-\phi_B^{x++}=\phi_B^{x+-}=\arg S_A^{x++}. \tag{9}$$

One can observe from Table I that the relationship (9) holds well in our experiment both for GaN and ZnSe.

The relations (7)–(8), which have been obtained from the 100% modulation and the π phase shift of the TI FWM signal in the (xxx) and (xyy) configuration, impose the following constrains on the PSF parameters:

$$C_{A,B}=\sqrt{\frac{v_{A,B}}{v_{B,A}}}C'. \tag{10}$$

These relations can be understood if one recalls that the PSF parameter C_A (C_B) can be interpreted as the ratio of the region occupied by σ_+-polarized $A(B)$ excitons to the volume, into which another σ_+-polarized $A(B)$ exciton can be excited. Similarly, the PSF parameter C' gives the ratio of the region occupied by an σ_+-polarized $A(B)$ excitons to the volume, into which a σ_--polarized $B(A)$ exciton can be excited. Being a composite particle, the $\sigma_\pm$-polarized A exciton consists of an electron with spin $\pm 1/2$ and a hole with spin $\mp 1/2$, while the $\sigma_\pm$-polarized B exciton consists of an electron with spin $\mp 1/2$ and a hole with spin $\mp 3/2$. Since the Pauli exclusion principle forbids two equivalent electrons and/or holes with the same coordinates, one can expect that two excitons cannot be excited simultaneously, regardless of the fact if one or two of their constituents have the same spin. Correspondingly, the reduction of the coupling of the $\sigma_+(\sigma_-)$-polarized A exciton with the relevant photon due to PSF is proportional to the total volume occupied by $\sigma_+(\sigma_-)$-polarized A excitons and $\sigma_-(\sigma_+)$-polarized B excitons, which include electrons with the same spin. One can readily find that the relation $C_A/C'=\sqrt{v_A/v_B}$ from Eq. (10) ensures this by reducing the interaction Hamiltonian (A1) to the following form:

$$H_A=-M_A b_{A+}^\dagger\left[1-\frac{C_A}{4V}(v_A b_{A+}^\dagger b_{A+}+v_B b_{B-}^\dagger b_{B-})\right]\mathcal{E}_+ - M_A b_{A-}^\dagger\left[1-\frac{C_A}{4V}(v_A b_{A-}^\dagger b_{A-}+v_B b_{B+}^\dagger b_{B+})\right]\mathcal{E}_- + \mathrm{h.c.} \tag{11}$$

In addition to the relationship (10) for the PSF factors, the 100% modulation and the π-phase shift of the TI FWM signal in the (xxx) and (xyy) configuration implies the following constrains on the memory functions, which describe the 2ω coherence in a system of two excitons with different valence orbitals:

$$F_{AA,BB}(t)=\sqrt{\frac{v_{A,B}}{v_{B,A}}}G_{AB}(t), \tag{12}$$

$$G_{AA,BB}(t)=\sqrt{\frac{v_{A,B}}{v_{B,A}}}F_{AB}(t). \tag{13}$$

In order to examine the implications of these constrains, one should recall that a memory function may consist of short- and long-memory correlation parts. In particular, the memory functions $F_{AA,BB}(t)$, which describe the interaction between excitons with the same energy and polarization, do not contain a long-memory part.[26] Therefore, Eq. (12) implies that $G_{AB}(t)$ also has no long-memory part, i.e., interaction between $\sigma_+(\sigma_-)$-polarized A excitons is described by the same (up to a constant factor, which depends on material parameters) memory function as the interaction between $\sigma_+(\sigma_-)$-polarized A excitons and $\sigma_-(\sigma_+)$-polarized B excitons. This indicates that—similar to the case discussed above—the memory functions are the same for excitons, which include electrons with the same spin. Therefore, the obtained constrains on the memory functions indicate a more important role of the electron spin in comparison to the hole spin for the exciton-exciton interaction. In the simplest approximation, if the correlation time is the shortest characteristic time in the system, the short-memory part can be written as $F_{AA}(t)=\sqrt{(v_A/v_B)}G_{AB}(t)=(v_A/v_B)F_{BB}(t)=(R'-iR'')\delta(t)$.

In contrast to excitons with parallel spins, the exciton memory function $G_{AA}(t)$, which describes the interaction be-

tween σ_+- and σ_--polarized A excitons and is of second- and higher-order in exciton-exciton interaction, consists of short- and long-memory parts.[26] The short-memory part is responsible for the correlation within the continuum of unbound two-exciton states, while the long-memory part describes the bound biexciton. If only A excitons would exist, the memory function could be written in the following form:[40,41] $G_{AA}(t)=W_A(t)-i\Delta G_A \exp\{i\omega_b^A t\}$. Here, $W_A(t)$ describes the short-memory correlations due to the continuum of unbound states, ω_b^A is the relevant biexcitonic binding energy. However, in the presence of two excitons with different valence orbitals, the structure of the two-exciton manifold may be complicated[42,43] depending on the material parameters. For example, mixed biexcitons,[43] which are formed from hh and lh excitons of same polarization have been observed in ZnSe QW.[42] From Eq. (13) one can see that the interaction between σ_+- and σ_--polarized A excitons is described by the same memory function as the interaction between σ_+-polarized A excitons and B excitons. By recalling that the electronic constituencies of the above exciton pairs are the same, one may conclude that the role of the electron spin in exciton-exciton interactions is more important in comparison to the hole spin.

C. Short-memory approximation

The above analysis of our experimental data, which accounts for the finite memory time of the four-particle correlation, allows us to obtain restraints (12,13) on the memory functions, which describe polarization-sensitive interactions between excitons. In particular, the combination of the phase and amplitude measurements of the beats in the TI FWM signal reveals that these general properties of the memory functions are responsible for the change in sign of the beating phase for the co- and counter-circular polarizations. However, the magnitude of the beating phase (9) is an integral characteristic. That is, the experimental measurement of the beating phase, which is a function of the memory depth and exciton dephasing rate, does not allow one to obtain the memory functions themselves. In order to reveal the temporal profile of the memory functions, time-resolved FWM measurements are necessary.

The relative contributions to the TI FWM signal from different mechanisms of coherent excitonic nonlinearity such as exciton-exciton interaction, EID and PSF can be estimated if the memory functions for the particular structure have been calculated using the dynamically controlled truncation scheme[44] or Hubbard operators approach.[26] However, the temporal profile of the memory functions, which is determined by the memory depth of the correlations in the continuum of unbound two-exciton states and the biexcitonic binding energy, may also be approximated on the basis of simple qualitative arguments[41] and/or experimental data. In this section, in order to clarify how the phase measurements can be employed to estimate the relative contributions from the different mechanisms to the excitonic nonlinearity, we consider the simplest, short-memory approximation. Specifically, we assume that the role of long-living correlations in one-exciton systems is not decisive,[34,40] i.e., that the long-living memory effects, which are associated with the biexciton state, do not play an important role in the TI FWM signal for our experimental conditions and may be accounted for by renormalizing the excitonic anharmonicity due to the continuum of unbound two-exciton states. Note that this approximation has allowed us to interpret the results of a frequency-domain FWM experiment in a strongly coupled exciton-cavity system.[28]

In the spirit of the short-memory approximation, we neglect the effects of the bound exciton states assuming

$$G_{AA}(t)=\sqrt{(v_A/v_B)}F_{AB}(t)$$
$$=(v_A/v_B)G_{BB}(t)=(W'-iW'')\delta(t),$$

where W' and W'' describe the exciton-exciton interaction and EID, respectively.[34] In such a case, the analysis developed in the Appendix gives $S_A^{x++}\propto(R'-iR''+3iC\gamma)(W'+iW'')$ and, correspondingly, from Eq. (9) one can derive

$$\phi_A^{x++}=\tan^{-1}\frac{(3C\gamma-R'')W'+R'W''}{R'W'-(3C\gamma-R')W''}. \tag{14}$$

If one assumes that in ZnSe and GaN $-W'>R',R''$ and $3\gamma C>R',R''$ (we have shown that these conditions are satisfied for the GaAs system[28]), Eq. (14) reduces to $\phi_A^{x++}\approx\tan^{-1}[-W'/W'']$. Correspondingly, the fact that $\phi_A^{x++}>0$ in Table I supports $W'<0$ for GaN and ZnSe (note, that the EID parameter $W''>0$ by definition). This implies that in these crystals σ_+- and σ_--polarized excitons of the same valence orbital attract one another, as well as two excitons of the same polarization and different valence orbitals. The measured value of the phase shift in the $(+++)$ configuration gives the relative amplitude of the anharmonicity of the low-density exciton gas due to exciton-exciton interaction and EID. Specifically, by using data from Table I, one can estimate $W''/(-W')\approx 0.7$ for GaN and $W''/(-W')\approx 3$ for ZnSe. That is despite the striking similarity of the signal in GaN and ZnSe of Figs. 2–5 the analysis of the beating phase reveals an important difference in the mechanism of the coherent optical nonlinearity in these materials. Specifically, one may expect the contribution from EID to the excitonic nonlinearity to be several times stronger in GaN than in ZnSe. Importantly, however, in ZnSe the role of the bound biexciton is known to be more pronounced in comparison to GaN. Correspondingly, one may expect that the biexciton states affects the ratio $W''/(-W')$ in ZnSe more strongly than in GaN. This, however, should be confirmed by time-resolved FWM measurements.

IV. CONCLUSION

We investigate the polarization dependence of the phase of the quantum beats in TI FWM signal in ZnSe and GaN. We observe phases of 0 and π for co- and cross-linear polarizations, respectively, at the resonance of the A (heavy-hole) and B- (light-hole) exciton for GaN (ZnSe). In co- and counter-circular polarizations, the observed phases of the beating signals are 0.2π (0.1π) and -0.2π (-0.1π) at the resonance of the A-exciton in GaN (heavy-hole exciton in

ZnSe), respectively. The phase of the signal changes sign when switching from the *A* to the *B* exciton in GaN (from the heavy- to the light-hole exciton in ZnSe). We describe the quantum beat process in the $\chi^{(3)}$ regime by accounting for memory effects in the nonlinear optical response at the fundamental band edge. It is shown that the interaction of excitons with different valence orbitals (e.g., *hh* and *lh* excitons) may be described by the same memory functions as the interaction of excitons with the same valence orbitals providing that the spin of the electronic constituents in both cases is the same. This implies that the excitonic anharmonicity can be classified in terms of the spins of the electrons forming the excitons rather than in the spin of the holes. In particular, the repulsive interaction between excitons with the same valence orbital and equal angular momentum implies a repulsion between excitons with different valence orbitals and opposite angular momenta. Similarly, since excitons with the same valence orbital and opposite angular momenta attract one another, excitons with different valence orbitals and the same angular momentum will also attract one another, giving rise to the formation of a mixed biexciton. Note that in contrast to biexcitons, which are formed from a pair of *hh* or *lh* excitons with opposite angular momentum and can be observed only in the (xxx), (xyy), and $(x+-)$ configurations, mixed biexcitons can be also observed in the $(+++)$ and $(x++)$ configurations.

It is necessary to emphasize that the striking similarity, which we observe in the quantum beat signal from GaN and ZnSe, originates from the strong influece of the four-particle correlation on the nonlinear optical response at the semiconductor band edge. In particular, the interaction between excitons with different valence orbitals, which is mainly determined by the spin of the electronic constituents, gives rise to the change of sign of the quantum beats phase when switching from the co- to the cross-circular polarization configuration. This property does not depend on the particular material, however, the magnitude of the beating phase is apparently material dependent. We demonstrate, in particular, that the difference in quantum beat phases, which we observe in ZnSe and GaN at positive time delay in the $(x++)$ and $(x+-)$ configurations, can be explained by the difference in relative contributions to the TI FWM signal from the exciton-exciton interaction and the EID effects for these semiconductors. This experimental finding, along with the developed theoretical description of the third-order optical effects at the fundamental band edge, makes the beating phase measurements a promising technique for the quantitative study of the four-particle correlation effects.

ACKNOWLEDGMENTS

We are grateful to H. Sunakawa and A. Usui of NEC Corporation, and Professor K. Ohkawa of the Science University of Tokyo for providing the samples. We would like to thank Dr. A.A. Yamaguchi and Dr. H. Suzuura for fruitful discussions. This work was partially supported by a grant-in-aid for COE Research of the Ministry of Education, Science, Sport and Culture of Japan.

APPENDIX: EVOLUTION EQUATION OF THE EXCITON POLARIZATION IN THE $\chi^{(3)}$ REGIME: MEMORY EFFECTS

In this Appendix, we introduce the major mechanisms of the coherent nonlinearity in a two-exciton system. We assume that two exciton resonances, which are labeled by subscripts *A* and *B*, are excited by an ultrashort laser pulse with frequency ω. The optical response of the two-exciton system at the frequency ω can be described by the complex amplitudes of the excitonic polarization associated with the *A* and *B* excitons, $P_{A,B\pm}e^{-i\omega t}=M_{A,B}\langle b_{A,B\pm}\rangle/V$, where $b_{A,B\pm}$ are the corresponding exciton annihilation operators (subscripts $\pm$ denote circular polarizations), $M_{A,B}$ are the exciton dipole moments, and V is the crystal volume. The angular brackets denote statistical averaging. The dipole moment of three-dimensional excitons is determined by the well-known relation $M_{A,B}=\mu_{A,B}(V/\pi a_{A,B}^3)^{1/2}$ where $\mu_{A,B}$ and $a_{A,B}$ are corresponding interband dipole moments and exciton Bohr radii, respectively. In order to make the analysis more transparent, we introduce the averaged interband dipole moment $\mu=\sqrt{\mu_A^2+\mu_B^2}$ and effective exciton volumes $v_{A,B}=\pi a_{A,B}^3(\mu/\mu_{A,B})^2$, which allows us to reduce the exciton dipole moments to $M_{A,B}=\mu(V/v_{A,B})^{1/2}$. In order to describe the PSF effect we write the exciton-photon coupling Hamiltonian[36] for the case of the two-exciton system as $H_{int}=H_A+H_B+\text{h.c.}$, where

$$H_A=-M_A b_{A+}^{\dagger}\left(1-\frac{v_A}{4V}C_A b_{A+}^{\dagger}b_{A+}-\frac{\sqrt{v_A v_B}}{4V}C' b_{B-}^{\dagger}b_{B-}\right)\mathcal{E}_+ - M_A b_{A-}^{\dagger}\times\left(1-\frac{v_A}{4V}C_A b_{A-}^{\dagger}b_{A-}-\frac{\sqrt{v_A v_B}}{4V}C' b_{B+}^{\dagger}b_{B+}\right)\mathcal{E}_- +\text{h.c.} \tag{A1}$$

Here, $\mathcal{E}_\pm$ are the circular components of the electric field of the light wave, while the PSF parameters C and C' describe the reduction of the exciton-photon coupling due to the finite excitation density. In terms of the few level models, C and C' are measures of the reduction of the dipole moment of the transitions $b_{A\pm}^{\dagger}0\rangle\rightarrow b_{A\pm}^{\dagger}b_{A\pm}^{\dagger}|0\rangle$ and $b_{A\pm}^{\dagger}0\rangle\rightarrow b_{A\pm}^{\dagger}b_{b\mp}^{\dagger}|0\rangle$ in comparison to $|0\rangle\rightarrow b_{A\pm}^{\dagger}|0\rangle$, respectively. Since in the states $b_{A\pm}^{\dagger}b_{A\pm}^{\dagger}|0\rangle$, both electrons and holes have the same angular momentum while in the states $b_{A\pm}^{\dagger}b_{B\mp}^{\dagger}|0\rangle$, only electrons have the same angular momentum, C and C' are generally different from one another. H_B can be obtained from H_A by replacing subscript *A* with *B* in Eq. (A1). By recalling that the free energy, associated with the light-matter interaction is given by $F=\langle H_{int}\rangle=-\mathcal{P}_+\mathcal{E}_+-\mathcal{P}_-\mathcal{E}_-$, where $\mathcal{P}_\pm$ are the circular components of the electric polarization in the medium, one can see from Eq. (A1) that when accounting for the PSF effect, the amplitude of the macroscopic polarization associated with the *A* exciton can be introduced as

$$P_{A\pm}=M_A\left\langle\left(1-\frac{v_A}{4V}C_A b^{\dagger}_{A\pm}b_{A\pm} - \frac{\sqrt{v_A v_B}}{4V}C' b^{\dagger}_{B\mp}b_{B\mp}\right)b_{A\pm}\right\rangle/V. \tag{A2}$$

We describe the coherent interaction between excitons by extending the treatment developed in Ref. 34 to the two-exciton case. The Hamiltonian, which describes the interaction between optically active excitons, can be written as $H_{xx}=H_{AA}+H_{BB}+H_{AB}$, where H_{AA} and H_{BB} describe the contribution to the total Hamiltonian arising from two-body interactions within ensembles of A and B excitons, while H_{AB} accounts for the interaction between them. H_{AA} consists of three terms:

$$H_{AA}=\tfrac{1}{2}\mathcal{B}^{++}_{AA}b^{\dagger}_{A+}b^{\dagger}_{A+}+\tfrac{1}{2}\mathcal{B}^{--}_{AA}b^{\dagger}_{A-}b^{\dagger}_{A-}+\mathcal{B}^{+-}_{AA}b^{\dagger}_{A+}b^{\dagger}_{A-} + \text{h.c.}, \tag{A3}$$

where the operators $\mathcal{B}^{++}_{AA}$ and $\mathcal{B}^{--}_{AA}$ describe the two-exciton coherence due to the interaction of A excitons with spin $\sigma=\pm1$, respectively, while $\mathcal{B}^{+-}_{AA}$ represents the two-exciton coherence due to the interaction of A excitons with opposite spin. The expectation values $\langle\mathcal{B}^{\pm\pm}_{AA}\rangle$ and $\langle\mathcal{B}^{+-}_{AA}\rangle$ give amplitudes for the 2ω coherence, which are due to unbound and bound two-exciton states with angular momenta $J_z=\pm2$ and $J_z=0$, respectively. Since the 2ω coherence arises from the relevant circular components of the excitonic polarization at the frequency ω, these amplitudes can be written from the causality principle as

$$\langle\mathcal{B}^{\pm\pm}_{AA}\rangle=\left(\frac{v_A}{\mu}\right)^2\int_0^{\infty}F_{AA}(\tau)P^2_{A\pm}(t-\tau)e^{-2i(\omega_A-\omega-i\gamma)\tau}d\tau, \tag{A4}$$

$$\langle\mathcal{B}^{+-}_{AA}\rangle=\left(\frac{v_A}{\mu}\right)^2\int_0^{\infty}G_{AA}(\tau)P_{A+}(t-\tau)\times P_{A-}(t-\tau)e^{-2i(\omega_A-\omega-i\gamma)\tau}d\tau,$$

where ω_A and γ are the A-exciton frequency and dephasing rate, respectively, while $F_{AA}(\tau)$ and $G_{AA}(\tau)$ are memory functions, which are associated with the interaction between two A excitons with equal and opposite spin, respectively. Similarly, the amplitude of the 2ω coherence associated with the interaction between B excitons can be described by the memory functions $F_{BB}(\tau)$ and $G_{BB}(\tau)$.

The coherent interaction between A and B excitons can be described by the following Hamiltonian:

$$H_{AB}=\mathcal{B}^{++}_{AB}b^{\dagger}_{A+}b^{\dagger}_{B+}+\mathcal{B}^{--}_{AB}b^{\dagger}_{A-}b^{\dagger}_{B-}+\mathcal{B}^{+-}_{AB}b^{\dagger}_{A+}b^{\dagger}_{B-} + \mathcal{B}^{-+}_{BA}b^{\dagger}_{A-}b^{\dagger}_{B+}+\text{h.c.}, \tag{A5}$$

where operators $\mathcal{B}^{\pm\pm}_{AB}$ and $\mathcal{B}^{\pm\mp}_{AB}$ describe the two-exciton coherence due to the interaction of A and B excitons with equal and opposite polarization, respectively. The expectation values $\langle\mathcal{B}^{\pm\pm}_{AB}\rangle$ and $\langle\mathcal{B}^{\pm\mp}_{AB}\rangle$ give the amplitudes of the 2ω coherence, which are due to the relevant bound and unbound two-exciton states with angular momenta $J_z=\pm2$ and $J_z=0$, respectively. These amplitudes can be written as the following:

$$\langle\mathcal{B}^{\pm\pm}_{AB}\rangle=\frac{v_A v_B}{\mu^2}\int_0^{\infty}F_{AB}(\tau)P_{A\pm}(t-\tau)\times P_{B\pm}(t-\tau)e^{-i(\omega_A+\omega_B-2\omega-2i\gamma)\tau}d\tau, \tag{A6}$$

$$\langle\mathcal{B}^{\pm\mp}_{AB}\rangle=\frac{v_A v_B}{\mu^2}\int_0^{\infty}G_{AB}(\tau)P_{A\pm}(t-\tau)\times P_{B\mp}(t-\tau)e^{-i(\omega_A+\omega_B-2\omega-2i\gamma)\tau}d\tau.$$

Here, the memory functions $F_{AB}(\tau)$ and $G_{AB}(\tau)$ describe the amplitude of the 2ω coherence associated with the interaction between A and B excitons with equal and different polarization, respectively.

The temporal evolution of the annihilation operators are given by the Heisenberg equation

$$-i\hbar\frac{\partial b_{A,B\pm}}{\partial t}+\hbar\omega_{A,B}b_{A,B\pm}=[H_{xx}+H_{int},b_{A,B\pm}]. \tag{A7}$$

By using Eqs. (A1), (A3), and (A5) one can find that the evolution equation for the exciton annihilation operator reduces to

$$\begin{aligned}-i\hbar\frac{\partial b_{A\pm}}{\partial t}+\hbar\omega_A b_{A\pm}=&-\mathcal{B}^{\pm\pm}_{AA}b^{\dagger}_{A+}-\mathcal{B}^{+-}_{AA}b^{\dagger}_{A\mp}\\&-\mathcal{B}^{\pm\pm}_{AB}b^{\dagger}_{B\pm}-\mathcal{B}^{\pm\mp}_{AB}b^{\dagger}_{B\mp}\\&+M_A\left(1-\frac{v_A}{2V}C_A b^{\dagger}_{A\pm}b_{A\pm}-\frac{\sqrt{v_A v_B}}{4V}C' b^{\dagger}_{B\mp}b_{B\mp}\right)\mathcal{E}_{\pm}\\&-M_A\frac{v_A}{4V}C_A b_{A\pm}b_{A\pm}\mathcal{E}_{\pm}\\&-M_B\frac{\sqrt{v_A v_B}}{4V}C' b^{\dagger}_{B\mp}b_{A\pm}\mathcal{E}_{\mp}\\&-M_B\frac{\sqrt{v_A v_B}}{4V}C' b_{B\mp}b_{A\pm}\mathcal{E}_{\mp}.\end{aligned} \tag{A8}$$

Statistical averaging and Eqs. (A2) and (A4) allow us to arrive at the following equation for the amplitude of the normalized optical polarization $p_{A\pm}=P_{A\pm}(v_A/\mu)$ at the frequency ω:

$$-i\frac{\partial p_{A\pm}}{\partial t}+\Delta_A p_{A\pm}=E_\pm-\left(C_A|p_{A\pm}|^2+\frac{1}{2}\sqrt{\frac{v_A}{v_B}}C'|p_{B\mp}|^2\right)E_\pm-\frac{1}{2}\sqrt{\frac{v_A}{v_B}}C'p^*_{B\mp}p_{A\pm}E_\mp$$
$$-p^*_{A\pm}\int_0^\infty F_{AA}(\tau)p^2_{A\pm}(t-\tau)e^{-2i\Delta_A\tau}d\tau-p^*_{B\pm}\sqrt{\frac{v_A}{v_B}}\int_0^\infty F_{AB}(\tau)p_{A\pm}(t-\tau)$$
$$\times p_{B\pm}(t-\tau)e^{-i(\Delta_A+\Delta_B)\tau}d\tau-p^*_{A\mp}\int_0^\infty G_{AA}(\tau)p_{A\pm}(t-\tau)p_{A\mp}(t-\tau)e^{-2i\Delta_A\tau}d\tau$$
$$-p^*_{B\mp}\sqrt{\frac{v_A}{v_B}}\int_0^\infty G_{AB}(\tau)p_{A\pm}(t-\tau)p_{B\mp}(t-\tau)e^{-i(\Delta_A+\Delta_B)\tau}d\tau. \quad \text{(A9)}$$

Here, $\Delta_{A,B}=\omega_{A,B}-\omega-i\gamma$, $\omega_{A,B}$, and γ are the exciton frequencies and dephasing rate, respectively, and $E_\pm$ are the Rabi frequencies, which corresponds to the amplitudes of the right- and left-circular components of the electric field at the frequency ω, $E_\pm e^{-i\omega t}+\text{c.c.}=\mu\mathcal{E}_\pm/\hbar$.

To clarify the meaning of the memory functions in Eq. (A9), let us consider the mean-field approximation, when only instantaneous interaction between excitons with the same spin and the same energy is allowed,[39] $F_{AA,BB}=R_{A,B}\delta(\tau)$, $F_{AB}(\tau)=G_{AA}(\tau)=G_{AB}(\tau)=0$ and $C'=0$. One can derive from Eq. (A9) that the evolution equation reduces to

$$-i\frac{\partial p_{A\pm}}{\partial t}+\Delta_A p_{A\pm}=(1-C_A|p_{A\pm}|^2)E_\pm-R_A|p_{A\pm}|^2p_{A\pm}. \quad \text{(A10)}$$

However, since in the coherent regime $\langle b^\dagger_\pm b_\pm\rangle=|\langle b_\pm\rangle|^2$, the excitonic polarization determines the population of excitons: $N_{A\pm}=|p_{A\pm}|^2/v_A$. This allows us to reduce Eq. (A10) to the standard modified semiconductor Bloch equation[45] for A excitons in terms of the normalized excitonic polarization, $p_{A\pm}$, and population, $n_{A\pm}=N_{A\pm}v_A$:

$$\frac{\partial p_{A\pm}}{\partial t}+[i(\omega_A-\omega)+\gamma]p_{A\pm}$$
$$=i\left(1-\frac{2n_{A\pm}}{n_{A0}}\right)E_\pm-\left(\sigma_A-i\frac{2\epsilon_A}{n_{A0}}\right)|p_{A\pm}|^2p_{A\pm}. \quad \text{(A11)}$$

Here we have introduced the exciton saturation density $n_{A0}=2/C_A$, the Lorentz shift of the exciton frequency $\epsilon_A=\text{Re}\{R_A\}/C_A$, and the EID correction to the exciton dephasing rate, $\sigma_A=-\text{Im}\{R_A\}$.[34]

We assume that the incident light pulses of duration τ_p with wave-vectors $\mathbf{k}_{1,2}$ are shorter than the exciton coherence time and use the δ-function approximation for the incident electric field:

$$E_\pm=E_{1\pm}\delta\left(\frac{t-\tau_1}{\tau_p}\right)\exp\{i\mathbf{k}_1\mathbf{r}\}+E_{2\pm}\delta\left(\frac{t-\tau_2}{\tau_p}\right)\exp\{i\mathbf{k}_2\mathbf{r}\}.$$

In this paper, we will consider the case of positive time delay, $T=\tau_1-\tau_2>0$, i.e., the pulse with wave-vector $\mathbf{k}_2$ arrives first. The exciton polarizations linear in $E_{1,2\pm}$ can be readily obtained as

$$p^{(1)}_{A(B)1,2\pm}=i\tau_pE_{1,2\pm}\exp\{-(i\Omega_{A(B)}+\gamma)\times(t-\tau_{1,2})\}\Theta(t-\tau_{1,2}),$$

where $\Theta(x)$ is the Heviside function, and $\Omega_{A,B}=\omega_{A,B}-\omega$.

The circular components of the nonlinear polarization associated with the wave propagating along the $2\mathbf{k}_1-\mathbf{k}_2$ direction can be obtained from the evolution Eq. (A9) as follows:

$$p^{(3)}_{A\pm}(t)=-\tau_p^3e^{-\gamma T}e^{-(i\Omega_A+\gamma)(t-\tau_1)}\Theta(t-\tau_1)\times\left\{\left[r_{AA}(t-\tau_1)e^{i\Omega_AT}+\sqrt{\frac{v_A}{v_B}}r_{AB}(t-\tau_1)e^{i\Omega_BT}\right]\times E^2_{1\pm}E^*_{2\pm}+\left[s_{AA}(t-\tau_1)e^{i\Omega_AT}+\sqrt{\frac{v_A}{v_B}}s_{AB}(t-\tau_1)e^{i\Omega_BT}\right]E_{1+}E_{1-}E^*_{2\mp}\right\}. \quad \text{(A12)}$$

Here $T=\tau_1-\tau_2$ and

$$r_{AA}(t)=iC_A+\int_0^te^{-2\gamma t'}\int_0^{t'}F_{AA}(t'')dt''dt',$$

$$r_{AB}(t)=\int_0^te^{-2\gamma t'}\int_0^{t'}F_{AB}(t'')dt''dt',$$

$$s_{AB}(t)=iC'+\int_0^te^{-2\gamma t'}\int_0^{t'}G_{AB}(t'')dt''dt',$$

$$s_{AA}(t)=\int_0^te^{-2\gamma t'}\int_0^{t'}G_{AA}(t'')dt''dt'.$$

$p^{(3)}_{B\pm}(t)$ can be obtained from Eq. (A12) by replacing subscript ''A'' with ''B.''

By using Eq. (A12), one can obtain the x component of the nonlinear polarization associated with the A exciton, $p_A^{(3)xst}(t)=[p_{A+}^{(3)}(t)+p_{A-}^{(3)}(t)]/\sqrt{2}$, for different polarizations of the pump and test waves, which are abbreviated by superscripts ''p'' and ''t,'' respectively. Specifically, when the pump and test wave are cocircularly polarized, $p_A^{(3),x++}(t)$ can be obtained from Eq. (A12) at $E_{1-}=E_{2-}=0$. In the $(x+-)$ configuration, i.e., when the pump and test wave are counter-circular polarized, $p_A^{(3),x+-}(t)=[p_{A+}^{(3)}(t)+p_{A-}^{(3)}(t)]/\sqrt{2}$ at $E_{1-}=E_{2+}=0$. Similarly, by substituting in Eq. (A12) $E_{1-}=E_{1+}=E_1/\sqrt{2}$, $E_{2-}=E_{2+}=E_2/\sqrt{2}$, and $E_{1-}=-E_{1+}=E_1/\sqrt{2}$, $E_{2-}=-E_{2+}=E_2/\sqrt{2}$ we arrive at the third-order polarization for the (xxx) and (xyy) configurations, respectively. Finally, in the $(+++)$ configuration $p_A^{(3)+++}(t)=p_{A+}^{(3)}(t)$ from Eq. (A12) at $E_{1-}=E_{2-}=0$. The equations for the third-order polarization, which is associated with the A exciton, in the various polarization configurations can be represented as follows:

$$p_A^{(3),x++}(t)\propto\left[r_{AA}(t-\tau_1)e^{i\Omega_A T}+\sqrt{\frac{v_A}{v_B}}r_{AB}(t-\tau_1)e^{i\Omega_B T}\right]\times e^{-\gamma T}e^{-(i\Omega_A+\gamma)(t-\tau_1)}\Theta(t-\tau_1), \tag{A13}$$

$$p_A^{(3),x+-}(t)\propto\left[s_{AA}(t-\tau_1)e^{i\Omega_A T}+\sqrt{\frac{v_A}{v_B}}s_{AB}(t-\tau_1)e^{i\Omega_B T}\right]\times e^{-\gamma T}e^{-(i\Omega_A+\gamma)(t-\tau_1)}\Theta(t-\tau_1), \tag{A14}$$

$$p_A^{(3),xxx}(t)=p_A^{(3),x++}(t)+p_A^{(3),x+-}(t), \tag{A15}$$

$$p_A^{(3),xyy}(t)=p_A^{(3),x++}(t)-p_A^{(3),x+-}(t), \tag{A16}$$

$$p_A^{(3),+++}(t)=2p_A^{(3),x++}(t). \tag{A17}$$

The obtained equations for the third-order polarization at the frequencies of the A and B excitons give us the time-integrated FWM signal

$$I_{A,B}^{pts}(T)\propto\int_{-\infty}^{+\infty}|p_{A,B}^{(3),pts}(t)|^2dt=[I_{0A,B}^{pts}+\mathrm{Re}\{S_{A,B}^{pts}\}\cos\Delta T\pm\mathrm{Im}\{S_{A,B}^{pts}\}\sin\Delta T]e^{-2\gamma T}. \tag{A18}$$

Here, $I_{0A,B}^{pts}$ and $S_{A,B}^{pts}$ take the following form for different polarization configurations:

$$I_{0A,B}^{x++}=\int_0^{+\infty}\left[|r_{AA,BB}(t)|^2+\frac{v_{A,B}}{v_{B,A}}|r_{AB}(t)|^2\right]e^{-2\gamma t}dt, \tag{A19}$$

$$S_{A,B}^{x++}=\sqrt{\frac{v_{A,B}}{v_{B,A}}}\int_0^{+\infty}2r_{AA,BB}(t)[r_{AB}(t)]^*e^{-2\gamma t}dt, \tag{A20}$$

$$I_{0A,B}^{x+-}=\int_0^{+\infty}\left[|s_{AA,BB}(t)|^2+\frac{v_{A,B}}{v_{B,A}}|s_{AB}(t)|^2\right]e^{-2\gamma t}dt, \tag{A21}$$

$$S_{A,B}^{x+-}=\sqrt{\frac{v_{A,B}}{v_{B,A}}}\int_0^{+\infty}2s_{AA,BB}(t)[s_{AB}(t)]^*e^{-2\gamma t}dt, \tag{A22}$$

$$I_{0A,B}^{xxx,xyy}=\int_0^{+\infty}\left[|r_{AA,BB}(t)\pm s_{AA,BB}(t)|^2+\frac{v_{A,B}}{v_{B,A}}|r_{AB}(t)\pm s_{AB}(t)|^2\right]e^{-2\gamma t}dt, \tag{A23}$$

$$S_{A,B}^{xxx,xyy}=\sqrt{\frac{v_{A,B}}{v_{B,A}}}\int_0^{+\infty}2[r_{AA,BB}(t)\pm s_{AA,BB}(t)]\times[r_{AB}(t)\pm s_{AB}(t)]^*e^{-2\gamma t}dt. \tag{A24}$$

One can readily find from the above equations that the $\chi^{(3)}$ regime imposes the following relationships between the parameters of the TI FWM signal in different polarization configurations (compare with Ref. 28):

$$2(I_{0A,B}^{x++}+I_{0A,B}^{x+-})=I_{0A,B}^{xxx}+I_{0A,B}^{xyy} \tag{A25}$$

$$2(S_{A,B}^{x++}+S_{A,B}^{x+-})=S_{A,B}^{xxx}+S_{A,B}^{xyy} \tag{A26}$$

The observed phases of the quantum beats in the (xxx) and (xyy) configuration allows us to conclude that in these polarization configurations $\mathrm{Im}\{S_{A,B}^{xxx}\}=\mathrm{Im}\{S_{A,B}^{xyy}\}=0$, $\mathrm{Re}\{S_{A,B}^{xxx}\}>0$, and $\mathrm{Re}\{S_{A,B}^{xyy}\}<0$. Moreover, since $\mathrm{Im}\{S_{A,B}^{xxx}\}=\mathrm{Im}\{S_{A,B}^{xyy}\}=0$, Eq. (A26) returns $\mathrm{Im}\{S_{A,B}^{x++}\}=-\mathrm{Im}\{S_{A,B}^{x+-}\}$.

The almost 100% modulation depth of the TI FWM signal in the (xxx) and (xyy) configurations implies $\mathrm{Re}\{S_{A,B}^{xxx}\}=I_{0A,B}^{xxx}$ and $\mathrm{Re}\{S_{A,B}^{xyy}\}=-I_{0A,B}^{xyy}$. By using expressions (A19)–(A24) one can arrive at

$$\int_0^{+\infty}\left|r_{AA,BB}(t)+s_{AA,BB}(t)-\sqrt{\frac{v_{A,B}}{v_{B,A}}}\times[r_{AB}(t)+s_{AB}(t)]\right|^2e^{-2\gamma t}dt=0, \tag{A27}$$

$$\int_0^{+\infty}\left|r_{AA,BB}(t)-s_{AA,BB}(t)+\sqrt{\frac{v_{A,B}}{v_{B,A}}}\times[r_{AB}(t)-s_{AB}(t)]\right|^2e^{-2\gamma t}dt=0. \tag{A28}$$

Since the underintegral functions in the above equations cannot be negative, we have to conclude that they are zero. Therefore, the π-phase shift of the quantum beats and the

100%-modulation depth of the FWM signal in the (xxx) and (xyy) configuration imply the following relationships:

$$r_{AA}(t)=\sqrt{\frac{v_A}{v_B}}s_{AB}(t),\quad s_{AA}(t)=\sqrt{\frac{v_A}{v_B}}r_{AB}(t), \tag{A29}$$

$$r_{BB}(t)=\sqrt{\frac{v_B}{v_A}}s_{AB}(t),\quad s_{BB}(t)=\sqrt{\frac{v_B}{v_A}}r_{AB}(t). \tag{A30}$$

Correspondingly, we arrive at the following constrains for the memory functions and PSF parameters:

$$F_{AA,BB}(t)=\sqrt{\frac{v_{A,B}}{v_{B,A}}}G_{AB}(t),$$
$$G_{AA,BB}(t)=\sqrt{\frac{v_{A,B}}{v_{B,A}}}F_{AB}(t),\quad C_{A,B}=\sqrt{\frac{v_{A,B}}{v_{B,A}}}C'. \tag{A31}$$

It is necessary to note that in contrast to the Eqs. (A25)–(A26), which reflect the third-order nature of the coherent excitonic nonlinearity associated with the four-particle correlation, restraints (A31) are essentially based on our experimental findings. Specifically, these are the π-phase difference and 100%-modulation depth of the beating signal in the (xxx) and (xyy) configuration, which hold well in our experimental condition. As it is shown in Sec. III of the paper, the obtained relationships between memory functions and PSF parameters imply that the electron spin influences the exciton-exciton interaction more than the hole spin.

*Present address: Siemens AG, ICN TR ON D T 2, 815359 Munich, Germany.
†Author to whom correspondence should be addressed.

[1] E. B. Alexandrov, Opt. Spektrosk. **14**, 496 (1963).
[2] J. N. Dodd, R. D. Kauland, and D. M. Warrington, Proc. Phys. Soc. London **84**, 176 (1964).
[3] V. Langer, H. Stolz, and W. von der Osten, Phys. Rev. Lett. **64**, 854 (1990).
[4] E. O. Göbel, K. Leo, T. C. Damen, J. Shah, S. Schmitt-Rink, W. Schäfer, J. F. Müller, and K. Köhler, Phys. Rev. Lett. **64**, 1801 (1990).
[5] K. Leo, E. O. Göbel, T. C. Damen, K. Köhler, and P. Ganser, Appl. Phys. Lett. **57**, 19 (1990).
[6] K. Leo, E. O. Göbel, T. C. Damen, J. Shah, S. Schmitt-Rink, W. Schäfer, J. F. Müller, K. Köhler, and P. Ganser, Phys. Rev. B **44**, 5726 (1991).
[7] S. Schmitt-Rink, D. Bennhardt, V. Heuckeroth, P. Thomas, P. Haring, G. Maidorn, H. Bakker, K. Leo, D.-S. Kim, J. Shah, and K. Köhler, Phys. Rev. B **46**, 10 460 (1992).
[8] K. Bott, O. Heller, D. Bennhardt, S. T. Cundiff, P. Thomas, E. J. Mayer, G. O. Smith, R. Eccleston, J. Kuhl, and K. Ploog, Phys. Rev. B **48**, 17 418 (1993).
[9] T. Saiki, K. Takauchi, K. Ema, M. Kuwata-Gonokami, K. Ohkawa, and T. Mitsuyu, Cryst. Growth. **138**, 805 (1994).
[10] E. J. Mayer, G. O. Smith, V. Heuckeroth, J. Kuhl, K. Bott, A. Schulze, T. Meier, S. W. Koch, P. Thomas, R. Hey, and K. Ploog, Phys. Rev. B **51**, 10 909 (1995).
[11] D. Weber, W. Petri, U. Woggon, C. F. Klingshirn, S. Shevel, and E. O. Göbel, Phys. Rev. B **55**, 12 848 (1997).
[12] T. Aoki, G. Mohs, T. Ogasawara, R. Shimano, M. Kuwata-Gonokami, and A. Yamaguchi, Opt. Express **1**, 364 (1997).
[13] A. J. Fischer, W. Shan, G. H. Park, J. J. Song, D. S. Kim, D. S. Yee, R. Horning, and B. Goldenberg, Phys. Rev. B **56**, 1077 (1997).
[14] A. Tookey, D. J. Bain, I. J. Blewett, I. Galbraith, A. K. Kar, B. S. Wherrett, B. Vögele, K. A. Prior, and B. C. Cavenett, J. Opt. Soc. Am. **15**, 64 (1998).
[15] H. Stolz, V. Langer, E. Schreiber, S. Permogorov, and W. von der Osten, Phys. Rev. Lett. **67**, 679 (1991).
[16] M. Koch, J. Feldmann, G. von Plessen, E. O. Göbel, P. Thomas, and K. Köhler, Phys. Rev. Lett. **69**, 3631 (1992).
[17] A. L. Smirl, M. J. Stevens, X. Chen, and O. Buccafusca, Phys. Rev. B **60**, 8267 (1999).
[18] V. G. Lyssenko, J. Erland, I. Balslev, K.-H. Pantke, B. S. Razbirin, and J. M. Hvam, Phys. Rev. B **48**, 5720 (1993).
[19] T. Aoki, G. Mohs, M. Kuwata-Gonokami, and A. A. Yamaguchi, Phys. Rev. Lett. **82**, 3108 (1999).
[20] H. Wang, K. Ferrio, D. G. Steel, Y. Z. Hu, R. Binder, and S. W. Koch, Phys. Rev. Lett. **71**, 1261 (1993).
[21] T. Saiki, M. Kuwata-Gonokami, T. Matsusue, and H. Sakaki, Phys. Rev. B **49**, 7817 (1994).
[22] P. Kner, S. Bar-Ad, M. V. Marquezini, D. S. Chemla, and W. Schäfer, Phys. Rev. Lett. **78**, 1319 (1997).
[23] K. B. Ferrio and D. G. Steel, Phys. Rev. Lett. **80**, 786 (1998).
[24] D. S.Chemla, in *Nonlinear Optics in Semiconductors I*, edited by R. K. Willardson, E. R. Weber, E. Garmiere, and A. Kost, Semiconductors and Semimetals Vol. 58 (Academic Press, San Diego, 1999).
[25] V. Chernyak and S. Mukamel, J. Opt. Soc. Am. B **13**, 1302 (1996).
[26] Th. Ostreich, K. Schonhammer, and L. J. Sham, Phys. Rev. Lett. **74**, 4698 (1995).
[27] Th. Ostreich, K. Schonhammer, and L. J. Sham, Phys. Rev. B **58**, 12 920 (1998).
[28] M. Kuwata-Gonokami, S. Inouye, H. Suzuura, M. Shirane, R. Shimano, T. Someya, and H. Sakaki, Phys. Rev. Lett. **79**, 1341 (1997).
[29] B. Mieck, H. Haug, H. W. A. Hugel, M. F. Heinrich, and M. Wegener, Phys. Rev. B **62**, 2686 (2000).
[30] O. M. Schmitt, L. Banyai, and H. Haug, J. Lumin. **87-9**, 168 (2000).
[31] A. Usui, H. Sunakawa, A. Sakai, and A. A. Yamaguchi, Jpn. J. Appl. Phys., Part 1 **36**, L899 (1997).
[32] S. Weiser, T. Meier, J. Möbius, A. Euteneuer, E. J. Mayer, W. Stolz, M. Hofmann, W. W. Rühle, P. Thomas, and S. W. Koch, Phys. Rev. B **61**, 13 088 (2000).

[33] D. Bennhardt, P. Thomas, R. Eccleston, E. J. Mayer, and J. Kuhl, Phys. Rev. B **47**, 13 485 (1993).
[34] M. Kuwata-Gonokami, T. Aoki, Yu. P. Svirko, R. Shimano, and Yu. P. Svirko, J. Lumin. **87–89**, 162 (2000).
[35] H. Suzuura, Yu. P. Svirko, and M. Kuwata-Gonokami, Solid State Commun. **108**, 289 (1998).
[36] Yu. P. Svirko, M. Shirane, H. Suzuura, and M. Kuwata-Gonokami, J. Phys. Soc. Jpn. **68**, 674 (1998).
[37] M. Shirane, C. Ramkumar, Yu. P. Svirko, H. Suzuura, S. Inouye, R. Shimano, T. Someya, H. Sakaki, and M. Kuwata-Gonokami, Phys. Rev. B **58**, 7978 (1998).
[38] O. Akimoto and E. Hanamura, J. Phys. Soc. Jpn. **33**, 1537 (1972).
[39] H. Haug and S. W. Koch. *Quantum Theory of the Optical and Electronic Properties of Semiconductors*, (World Scientific, Singapore, 1993).
[40] Yu. P. Svirko and M. Kuwata-Gonokami, Phys. Rev. B **69**, 6912 (2000).
[41] L. J. Sham and Th. Ostreich, J. Lumin. **87–89**, 179 (2000).
[42] D. Birkedal, J. Singh, V. G. Lyssenko, J. Erland, and J. M. Hvam, Phys. Rev. Lett. **76**, 672 (1996).
[43] H. P. Wagner, W. Langbein, and J. M. Hvam, Phys. Rev. B **59**, 4584 (1999).
[44] V. M. Axt and A. Stahl, Z. Phys. B: Condens. Matter **93**, 195 (1994).
[45] M. Wegener, D. S. Chemla, S. Schmitt-Rink, and W. Schäfer, Phys. Rev. A **42**, 5675 (1990).